Two-Dimensional Structures of Crystalline Self-Aggregates of Amphiphilic Alcohols at the Air-Water Interface As Studied by Grazing Incidence Synchrotron X-ray Diffraction and Lattice Energy Calculations§

Jinn-Lung Wang,† Franck Leveiller,† Didier Jacquemain,† Kristian Kjaer,*,‡ Jens Als-Nielsen,*,‡ Meir Lahav,*,† and Leslie Leiserowitz*,†

Contribution from the Department of Materials and Interfaces, Weizmann Instituteof Science, Rehovot 76100, Israel, and Physics Department, RISØ National Laboratory, DK4000 Roskilde, Denmark

Received June 17, 1993®

Abstract: The two-dimensional (2D) crystal structures of self-aggregated clusters of amphiphilic alcohols ($C_nH_{2n+1}OH$, n = 23, 30, 31, and $C_{19}H_{39}CO_2(CH_2)_nOH$, n = 9, 10) on pure water at a temperature of 5 °C have been determined to near-atomic resolution in order to understand the relative abilities of these monolayers to induce ice nucleation. The structures were solved making use of grazing incidence synchrotron X-ray diffraction (GID) data, complemented by lattice energy calculations. The GID data of the different monolayers within each of the two series ($C_nH_{2n+1}OH$, $C_{19}H_{39}CO_2C_nH_{2n}OH$) are very similar. The molecules pack in a rectangular unit cell of average dimensions a = 5.0 Å, b = 7.5 Å for the *normal* alcohols $C_nH_{2n+1}OH$ and a = 5.7 Å, b = 7.5 Å for $C_{19}H_{39}CO_2CnH_{2n}OH$. The plane group symmetry is essentially $p1g1$ for the *normal* alcohols $C_nH_{2n+1}OH$ and essentially $p11g$ for the other group. The molecular chains are tilted from the vertical by an average angle of 9°, in the direction of the b axis, for $C_nH_{2n+1}OH$ and by 29°, in the direction of the a axis, for the other molecular type. The molecular chains related by glide (g) symmetry are arranged in a herringbone pattern. The fit to the Bragg rod intensity data of $C_nH_{2n+1}OH$ permitted a reliable estimate of 0.07 Å^2 for the molecular mean-squared motion parallel to the water surface. The absolute orientations of the molecules $C_{19}H_{39}CO_2C_nH_{2n}OH$ were determined by lattice energy calculations. The anisotropic coherence lengths of the crystallites of $C_{19}H_{39}CO_2C_nH_{2n}OH$ derived from the widths of the two observed Bragg peaks have been correlated with the binding energies of molecules in different directions.

1. Introduction

Recently we demonstrated that amphiphilic long-chain alcohols $C_nH_{2n+1}OH$ arranged in monolayers at the surface of water drops have the ability to promote ice nucleation.[1] The temperature of freezing of these water drops was found to be dependent upon both the length of the hydrocarbon chain and the parity of n, the number of carbon atoms in the chain. For the odd series, the freezing temperature rose from −11 to 0 °C on increasing the chain length from n = 17 to 31; for the even series the freezing point leveled off at a temperature of −8 °C, with n in the range 22–30. The ice-nucleating effect was accounted for by an assumed spontaneous formation of ordered two-dimensional (2D) clusters of alcohol molecules at the water surface,[1] with lattice dimensions close to those of the ab lattice of hexagonal ice. It was therefore deemed necessary to obtain direct information on the molecular packing of these amphiphiles to test this proposed mechanism.

In a previous paper[2] we reported results of a general nature on grazing incidence X-ray diffraction (GID) measurements using synchrotron radiation on uncompressed monolayers of three alcohols $C_nH_{2n+1}OH$, with different chain lengths and parities (n = 23, 30, 31) over water at 5 °C. The measurements, described here in part 6.1, indicated a high degree of lateral crystalline order for all three monolayers. The coherence lengths[3] L of the 2D crystallites of the monolayers were anisotropic in the range 250 and 1000 Å.

The measured GID patterns for the three alcohol monolayers (n = 23, 30, 31) were similar but for minor differences in peak positions. The Bragg peaks for the three monolayers are shown in Figure 1. The three observed Bragg reflections for each monolayer were indexed as {1,1} + {1,$\bar{1}$}, {0,2}, and {2,0} for a rectangular cell,[2] and the resulting unit cell parameters are listed in Table 1. The positions of the maxima of the Bragg rod intensity profiles of the three reflections indicated that the molecular axis lies approximately in a plane perpendicular to the short a axis of the unit cell, with an average tilt angle of 9° from the surface normal (Table 1).

The packing arrangements of the hydrocarbon chains were deduced from the 3D crystal structures of long-chain alcohols and alkanes. Such molecules adopt a layer structure,[4-6] in which neighboring hydrocarbon chains are related by glide symmetry, forming a herringbone arrangement, generally specified as the orthorhombic orthogonal ($O_\perp$) motif.[4,6] The dimensions of the cell perpendicular to the molecular axis are 4.98 by 7.42 Å. The dimensions of the unit cell for the alcohol monolayers projected along the molecular chain axis (Table 1) match well with those of the orthorhombic subcell of the 3D crystal structures. Thus we proposed[2] that in the monolayer crystallites of $C_nH_{2n+1}OH$ (n = 23, 30, 31) the chains pack in a primitive rectangular cell in which the molecules are tilted in the b direction and related to each other by a glide perpendicular to the a axis, in the symmetry plane group $p1g1$.

† Weizmann Institute of Science.
‡ RISØ National Laboratory.
§ Dedicated to Sir John Meurig Thomas on his 60th birthday.
® Abstract published in *Advance ACS Abstracts*, January 1, 1994.

(1) Gavish, M.; Popovitz-Biro, R.; Lahav, M.; Leiserowitz, L. *Science* **1990**, *250*, 973.
(2) Jacquemain, D.; Leveiller, F.; Weinbach, S.; Lahav, M.; Leiserowitz, L.; Kjaer, K.; Als-Nielsen, J. *J. Am. Chem. Soc.* **1991**, *113*, 7684-7691.
(3) Guinier, A. *X-ray Diffraction*; Freeman: San Francisco, CA, 1968.
(4) Abrahamsson, S.; Dahlén, B.; Löfgren, H.; Pascher, I. *Progress in the Chemistry of Fats and Other Lipids*; Pergamon Press: New York, 1978; Vol. 16, pp 125.
(5) Kitaigorodski, A. I. *Organic Chemical Crystallography*; Consultants Bureau Press: New York, 1961; Chapter 4.
(6) Small, D. M. *Handbook of Lipid Research*; *Plenum* Press: New York, 1986; Vol. 4, Chapters 2, 5, and 8.

0002-7863/94/1516-1192$04.50/0

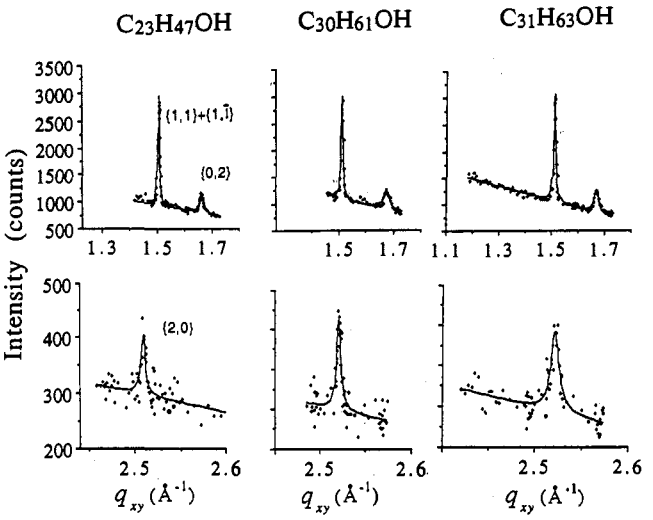

Figure 1. Observed Bragg diffraction peaks for {1,1} + {1,$\bar{1}$}, {0,2}, and {2,0} reflections across the horizontal scattering vector $\mathbf{q}_{xy}$ for the alcohol monolayers ($C_nH_{2n+1}OH$, n = 23, 30, 31).

Table 1. Results[a] of Bragg Peak Analysis for the Alcohol Monolayers $C_nH_{2n+1}OH$, n = 23, 30, 31

compd	d_{11},$d_{\bar{1}1}$ (Å) L (Å)	d_{02} (Å) L (Å)	d_{20} (Å) L (Å)	a (Å) (a_p)	b (Å) (b_p)	A (Å^2)	t (deg)
n = 23	4.18	3.78	2.50	5.00	7.56	18.90	9.5
	≥1000	360	≥1000	(5.00)	(7.46)		
n = 30	4.15	3.75	2.49	4.99	7.49	18.69	7.7
	≥1000	230	≥1000	(4.99)	(7.42)		
n = 31	4.16	3.77	2.49	4.99	7.53	18.79	10.1
	≥1000	270	700	(4.99)	(7.41)		

[a] t = tilt angle of monolayer molecules from the normal to the water surface. L = coherence length (Å) of the crystallites, determined using the Scherrer formula.[3] a and b are the lengths of the unit cell axes; a_p and b_p are the lengths of the unit cell projected along the molecular chain axis. In these systems, $a_p = a$ and $b_p = b \cos t$. A = area per molecule = $ab/2$.

In order to obtain a more definitive picture of the molecular packing of the alcohol monolayers at the air–water interface, we adopted a procedure described in a preceding paper[7] for pinpointing 2D crystal structures, involving an analysis of the Bragg rods complemented by lattice energy computations of a variety of possible packing arrangements.

We were faced with the question not only as to the precise packing of the alcohol chains in the 2D crystals of $C_nH_{2n+1}OH$ (n = 23, 30, 31) but also as to the conformation of their hydroxyl head groups. Indeed the GID data from 2D crystallites is not sufficiently sensitive to minor differences in molecular conformation at the head-group level. According to IR spectroscopy and X-ray diffraction data, the 3D crystals of the normal higher alcohols $C_nH_{2n+1}OH$ ($n > 15$) appear in either the γ or β forms.[8-10] In the γ form, all the alcohol chains adopt an all-trans conformation. They are tilted at an angle of approximately 35° from the axis perpendicular to the crystal layer and are arranged in the orthogonal ($O_\perp$) motif. The molecular chains in the β form are almost perpendicular to the crystal layer, as indicated by the crystal structure of 1-heptanedecanol[8,11] ($C_{17}H_{35}OH$), and are also arranged in the orthogonal ($O_\perp$) motif. In contrast to the case of the γ form, the conformation of the terminal C_α-OH group is gauche about the C_β–C_α bond for half the number of molecules and trans for the other half. Theoretical studies examining the interface between a hexanol monolayer and water predict that an average of two water molecules form hydrogen bonds with each hexanol molecule.[12] They also indicate that the terminal C–OH bond of the C–C–C–OH moiety can be in a trans or gauche conformation with equal probability. Thus we performed X-ray diffraction measurements on single 3D crystals of the following alcohols, $HO(CH_2)_9OH$, $HO(CH_2)_{10}OH$, $C_{24}H_{49}OH$, and $C_{25}H_{51}OH$, in order to extract more information on the conformation of the terminal head group, as described in parts 6.2 and 6.3.

The freezing point studies on water drops covered with monolayers were extended, as described in an accompanying paper,[13] making use of alcohols with functional groups such as secondary amide (CONH) or carboxy ester (CO_2) groups inserted in the chain to help induce packing arrangements different from those of the normal alcohols.

Monolayers of hydroxy alkyl esters of eicosanoic acid $C_{19}H_{39}CO_2(CH_2)_nOH$, n = 9, 10, were found to induce ice nucleation[13] although not as effectively as the normal long-chain alcohols. The monolayers of the hydroxy alkyl esters with n = 10 induce ice nucleation at a higher temperature than those with n = 9. On the assumption that the molecular chains are strongly tilted to the normal of the water surface, these results suggested that the difference in ice-nucleating temperature may be associated with a difference in alcohol OH orientation with respect to the water surface, provided the absolute orientation of the molecular chain is the same for the two molecules $C_{19}H_{39}CO_2(CH_2)_nOH$, n = 9, 10. The presence of the carboxy group (CO_2) in the molecular chain should allow us to fix the orientation of the molecule and so that of the OH head group with respect to the water surface. Thus we also performed GID measurements using synchrotron X-radiation on 9-hydroxynonyl eicosanoate (HNE, $C_{19}H_{39}CO_2(CH_2)_9OH$) and 10-hydroxydecyl eicosanoate (HDE, $C_{19}H_{39}CO_2(CH_2)_{10}OH$), as described in part 6.1.

2. Methodology of 2D Structure Determination

Here we describe the methodology adopted to determine the 2D crystal structures of the alcohol monolayers making use of the GID data and lattice energy calculations.[7]

The Bragg rod intensity profile can be expressed in terms of the molecular X-ray structure factor as follows

$$I_{hk}(q_z) = KLPA_{ABCD}A_{\text{cell}}^{-2}V(q_z)|F_{hk}(q_z)|^2DW_{hk}(q_z) \quad (1)$$

The observed Bragg rod intensity is actually a sum over those (h,k) reflections whose Bragg rods coincide at a particular horizontal $2\theta_{hk}$ angle, or q_{hk} position, where $q_{hk} = 4\pi \sin \theta_{hk}/\lambda$. In eq 1, the most important variation is due to the square of the molecular structure factor $|F_{hk}(q_z)|^2$. The Debye–Waller factor $DW_{hk}(q_z) = \exp -(q_{hk}^2U_{xy} + q_z^2U_z)$, where U_{xy} and U_z are respectively the mean-square amplitudes parallel and perpendicular to the monolayer plane. They account for the thermal motion of the atoms[14,15] in the molecule, as well as for ripples on the water surface, which lead to roughness of the interface.[16-18]

(7) Leveiller, F.; Jacquemain, D.; Leiserowitz, L.; Kjaer, K.; Als-Nielsen, J. *J. Phys. Chem.* **1992**, *96*, 10380.
(8) Tasumi, M.; Shimanouchi, T.; Watanabe, A.; Goto, R. *Spectrochim. Acta* **1964**, *20*, 629.
(9) Watanabe, A. *Bull. Chem. Soc. Jpn.* **1963**, *36*, 336.
(10) Wilson, D. A.; Ott, E. *J. Chem. Phys.* **1934**, *2*, 231.
(11) ONly the cell parameters and a figure of the crystal structure of 1-heptadecanol have been published[8] but without atomic coordinates.
(12) Gao, J.; Jorgensen, W. L. *J. Phys. Chem.* **1988**, *92*, 5813.
(13) Popovitz-Biro, R.; Wang, J. L.; Majewski, J.; Leiserowitz, L.; Lahav, M. *J. Am. Chem. Soc.*, preceding paper in this issue.
(14) Dunitz, J. D. *X-ray analysis and the structure of molecules*; Cornell University Press: Ithaca, NY, 1979; pp 43–49.
(15) In general, molecular thermal vibrations in crystals are anisotropic, which leads to a dependence of the corresponding temperature factor on the direction of the scattering vector.[14] For a 2D crystal lying in the xy plane, the extent of GID data can, in favorable cases, allow the temperature factor U to be decomposed into an in-plane U_{xy} and out-of-plane U_z component. Then, the Debye–Waller term $DW_{hk}(q_z)$ in eq 1 can be written $DW_{hk}(q_z) = \exp -(q_{hk}^2U_{xy} + q_z^2U_z)$, where $\mathbf{q} = \mathbf{q}_{hk} + \mathbf{q}_z$.
(16) Als-Nielsen, J.; Kjaer, K. In *Proceedings of the Nato Advanced Study Institute, Phase Transitions in Soft Condensed Matter*; Riste, T., Sherrington, D., Eds.; Plenum Press: New York, Gello, Norway, 1989; pp 113.
(17) Braslau, A.; Pershan, P. S.; Swislow, G.; Ocko, B. M.; Als-Nielsen, J. *Phys. Rev.* **1988**, *A38*, 2457.
(18) Pershan, P. S. *J. Phys. Colloq.* **1989**, *50*, 1.

The grazing geometry factor $V(q_z)$ describes the interference between the waves which are diffracted up from the monolayer and those that are diffracted down and subsequently reflected up;[19,20] it is seen as a sharp peak at $q_z \approx 0.01$ Å^{-1}. The corrections for crossed-beam area A_{ABCD}, depicted in the Experimental Section and in Figure 18 ($A \propto 1/\sin 2\theta_{hk}$), Lorentz ($L \propto 1/\sin 2\theta_{hk}$), and polarization ($P = \cos^2 2\theta_{hk}$) have been inserted; A_{cell} is the area of the unit cell. The factor K scales the calculated to the observed intensity.

The scarcity of observable Bragg rod data, due in part to the fact that the monolayers at the water surface are composed of a 2D crystalline "powder",[21] imposed a model with a small number of adjustable parameters. Thus we have refined the alcohol chain as a rigid body with one positional parameter (translation along the x or y direction depending upon the crystal symmetry) and three orientational parameters defined by the Eulerian angles ω, t, and ϕ.[22,23] The various model structures were each refined and eventually compared by the fitting of their calculated Bragg rod intensity profiles to the observed measurements. Molecular models on the atomic scale of the alcohols $C_nH_{2n+1}OH$ (n = 23, 30, 31) were constructed making use of low-temperature 3D single-crystal structures of normal aliphatic alcohols and diols, presented in this paper (see parts 6.2 and 6.3). The crystal structure of the diol $HO(CH_2)_9OH$ was used to construct the gauche conformation adopted by the C_α–OH group. The carbon skeleton of the all-trans chain was assumed to be coplanar.

The molecules of $C_{19}H_{39}CO_2C_nH_{2n}OH$, n = 9, 10, namely HNE and HDE, were assumed to adopt an all-trans conformation for the two hydrocarbon segments, in accordance with the 3D crystal structure of ethyl stearate.[24] The geometry of the ester moiety was taken from the crystal structures of 4-oxo-2-butenoic acid alkyl esters.[25] The conformation of the ester segment C–C–CO–O–C was assumed to be all-trans in accordance with observation.[26]

Atom–atom potential energy calculations which have proven to be an alternative method for confirmation or indeed ab initio prediction of possible 3D crystal structures,[27,28] were also applied as a complementary method for the 2D structure elucidation. The van der Waals parameters for each pair of atoms for the lattice energy calculations were taken from the results derived by Lifson, Hagler, and co-workers.[28] The electrostatic parameters in the form of net charges and dipole and quadrupole moments on each atom for the Coulomb energy calculations were extracted from the electron density deformation distribution derived from a low-temperature X-ray diffraction study of 1,3-diethylbicyclobutane-*exo*,*exo*-2,4-dicarboxylic acid.[29] The parameters pertaining to the atoms of the carboxyl moiety in this compound were used for the corresponding atoms of the carboxy ester moiety CO_2 in the HNE and HDE molecules. Since no analogous data of an alcohol were available, the electrostatic parameters of the alcohol hydroxyl group were derived from the atomic moments of a water molecule from a low-temperature X-ray diffraction study of cytosine monohydrate.[30]

The feasibility of obtained meaningful results in monolayers from such a procedure has already been demonstrated[7] by a determination of the 2D crystal structure of an uncompressed monolayer of $C_{29}H_{59}CO_2H$ over pure water at a temperature of 5 °C.

3. Results on Monolayers of the $C_nH_{2n+1}OH$ Series

3.1. Comparison of the Various Possible 2D Packing Arrangements. We shall first construct possible packing arrangements of the $C_nH_{2n+1}OH$ molecules assuming the planar all-trans conformation of the carbon skeleton and that the molecules pack in a rectangular cell and are tilted by 9° from the vertical in the direction of the b axis. The feasible 2D plane groups[31] for a rectangular unit cell are $c1m1$, $p2mg$, $p11g$, $p1g1$. The plane group $c1m1$ describes a translational packing in which parallel molecules lie on a mirror plane in a c-centered cell (Scheme 1a). The plane group $p2mg$ imposes a similar mirror constraint, but the glide plane, which is perpendicular to the mirror plane, induces the molecules to tilt in alternating directions to the mirror plane (Scheme 1b). With plane group $p11g$ the mirror constraint is dropped but leaves the molecules to tilt in alternating directions (Scheme 1c). In the case of plane group $p1g1$, all the molecular chain axes are parallel, but not the planes through the molecules related by glide symmetry (Scheme 1d). There does remain the possibility of an oblique, primitive cell $p1$, but where the nonsymmetry-related {1,0} and {0,1} reflections corresponding to the basal reciprocal axes coincide to yield a unit cell in real space, which may be expressed as a c-centered rectangular with symmetry $c1$, as shown in Scheme 1e.

Employing eq 1, the intensity profiles of the Bragg rods corresponding to the three measured reflections {1,1} + {1,$\bar{1}$}, {0,2}, and {2,0} of each of the three 2D crystalline powders were calculated using atomic coordinate models of the $C_nH_{2n+1}OH$ (n = 23, 30, 31) molecules. So as to generate all possible 2D crystal structures with plane symmetries $p11g$ and $p2mg$ (which is a special case of $p11g$), the molecules were given full rotation about their long axes and translated along the b axis from $y = -0.25$ to $+0.25$ (the glide plane is at $y = \pm 0.25$).[32] The ratio of the calculated intensities of the two reflections $I_{\{0,1\}}$:$I_{\{1,1\}+\{1,\bar{1}\}}$, integrated along the vertical scattering vector q_z of the Bragg rod, varies in the range 2.3–4.7. These results are incompatible with the GID measurements: the {0,1} reflection was not observed (Table 2), and the intensity of the {1,1} + {1,$\bar{1}$} reflection is strong (Figures 1 and 3). Thus we dismiss the two plane groups $p11g$ and $p2mg$. For the plane groups $p1g1$ and $c1$, the molecules were given a full rotation in ϕ about their chain axes, so as to generate all feasible packing arrangements. The results of the structure-factor

(19) Vineyard, G. *Phys. Rev. B* **1982**, *26*, 4146–4159.
(20) Feidenhans'l, R. *Surf. Sci. Rep.* **1989**, *10* (3), 105.
(21) In all the grazing incidence diffraction patterns measured to date, the monolayers were found to be composed of crystallites randomly oriented on the water surface, forming a 2D "powder".
(22) Goldstein, H. *Classical Mechanics*; Addison-Wesley: Cambridge, MA, 1980.
(23) The Eulerian angles were specified according to the convention given by Goldstein[22] but where ω, t, and ϕ replace the angles φ, θ, and ψ, respectively. The following convention was used to describe the orientation of the molecule at the starting position $\omega = t = \phi = 0°$: the molecular chain is parallel to the vertical c axis, and the plane through the carbon chain is parallel to the ac plane. ω is a rotation of the molecule about the vertical axis, t is the angle of tilt from the vertical, and ϕ is the rotation of the molecule about its long axis.
(24) Aleby, S. *Acta Chem. Scand.* **1968**, *22*, 811–818.
(25) Glowka, M. L.; Iwanicka, I. *Acta Crystallogr.* **1990**, *C46*, 1262–1264; **1991**, *C47*, 618–620.
(26) Dunitz, J. D.; Strickler, P. In *Structural Chemistry and Molecular Biology*; Rich, A.; Davidson, N., Eds.; Freemna: San Francisco, CA, 1968; pp 595–602. Leiserowitz, L.; Schmidt, G. M. J. *Acta Crystallogr.* **1965**, *18*, 1058.
(27) Williams, D. E.; Starr, T. L. *Comput. Chem.* **1977**, *1*, 173. Leiserowitz, L.; Hagler, A. T. *Proc. R. Soc. London* **1983**, *A388*, 133. Pertsin, A. J.; Kitaigorodski, A. I. *The Atom–Atom Potential Method*; Springer-Verlag: Berlin, 1987. Gavezzotti, A. *J. Am. Chem. Soc.* **1991**, *113*, 4622. Karfunkel, H. R.; Gdanitz, R. J. *J. Comput. Chem.* **1992**, *13*, 1171.
(28) Lifson, S.; Hagler, A. T.; Dauber, P. *J. Am. Chem. Soc.* **1979**, *101*, 5111–5121.
(29) Eisenstein, M.; Hirshfeld, F. L. *Acta Crystallogr.* **1983**, *B39*, 61.
(30) Eisenstein, M. *Acta Crystallogr.* **1988**, *B44*, 412.
(31) *International Tables for X-ray Crystallography*; Kynoch Press: Birmingham, England, 1965; Vol. 1.
(32) Reasonable intermolecular contact is only possible if the central axis of the molecule lies on a place halfway between neighboring glide planes. Thus the x coordinate of the molecular axis is fixed at $x = 0$.
(33) The deviation from a perfect rectangular unit cell is given by the deviation $\Delta\gamma$ of the angle γ from 90°. This deviation is measured by the difference between the position of the {1,1} reflection and that of the {1,$\bar{1}$} reflection. Because the width of the {1,1} + {1,$\bar{1}$} reflection is very close to the resolution limit as determined by the Soller collimator, a split would have been observable with $\Delta\gamma$ as low as 0.3°. Thus within the limits of experimental error, the cell is rectangular. We may envisage a $c1$ cell only when the plane through the carbon chain is parallel to the ac plane namely at $\phi = 0°$, as was derived for the 2D crystal structure of arachidamide monolayers.[34]

Scheme 1

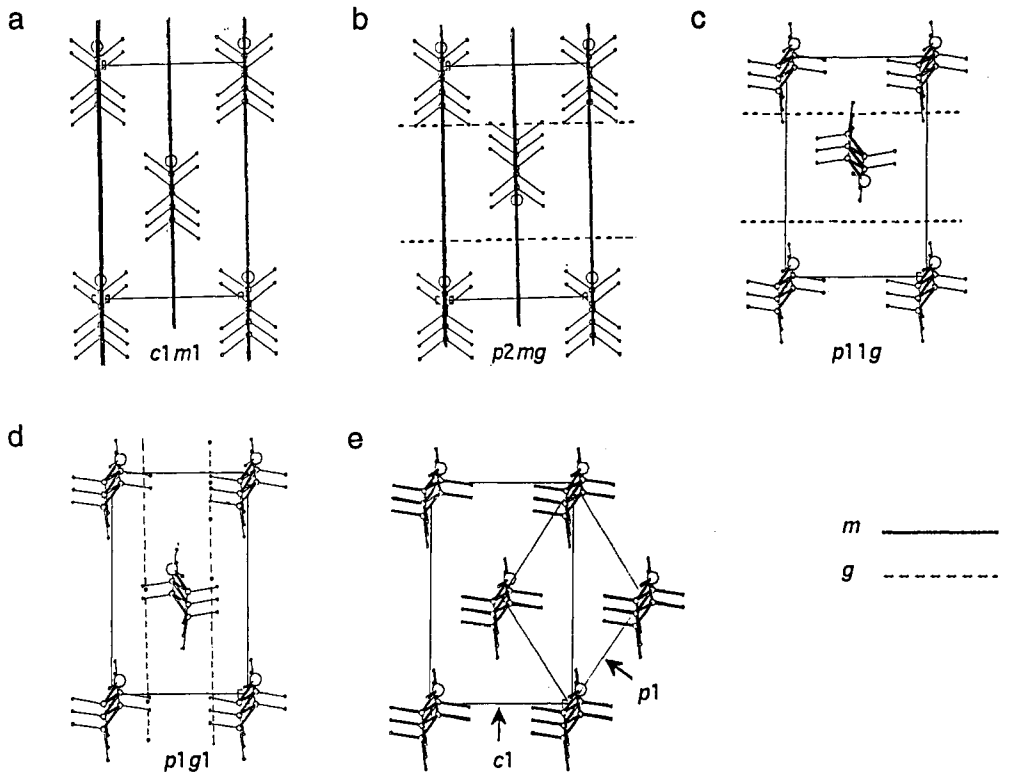

Table 2. Observed and Calculated GID Data of the Monolayer of $C_{31}H_{63}OH$[a]

				I_c						
hk	*d* (Å)	q_{xy} (Å^{-1})	I_o	*p*1*g*1	*c*1*m*1	*p*11*g*	*p*2*mg*	*c*1	model I	model II
{0,1}	7.54	0.83	<3[b]	*c*	*c*	100	100	*c*	0.1	8.1
{0,2}	3.77	1.67	29.5	35.5	15.7	9.1	6.0	30.3	34.3	32.1
{0,3}	2.51	2.50	<3[b]	*c*	*c*	1.1	0.2	*c*	0.1	0.4
{1,$\bar{2}$} + {1,2}	3.01	2.09	<3[b]	1.9	*c*	4.3	4.7	*c*	1.8	3.0
{1,$\bar{1}$} + {1,1}	4.16	1.51	100	100	100	25.1	31.6	100	100	100
{1,0}	4.99	1.26	<3	0.1	*c*	*c*	*c*	*c*	0.3	0.7
{2,0}	2.49	2.54	4.2	5.2	7.3	3.4	4.7	6.0	4.5	4.7

[a] Included are the observed (I_o) and calculated (I_c) intensities of the Bragg peaks for the various model structures on a relative scale. The intensities were calculated with molecular tilt angle $t = 10°$ and a rotation angle about the molecular axis $\phi = 45°$ for the plane groups *p*1*g*1, *p*11*g*, and *c*1. $q_{xy} = 4\pi \sin\theta/\lambda$ is the horizontal scattering vector. Model I is the pseudo *p*1*g*1 glide model with an all-trans molecular conformation. Model II is the pseudo *p*1*g*1 glide model in which the unit cell contains one molecule with the all-trans conformation and the other molecule with an end-of-chain C–OH *gauche* conformation. [b] These reflections were unobserved. Intensities estimated to be <3. [c] A symmetry forbidden reflection.

calculations pertaining to the three observed reflections were expressed in terms of the reliability fit indices $R = \sum|I_o - I_c|/\sum I_o$ and $R_w = \sum w|I_o - I_c|/\sum wI_o$, where I_o and I_c are the observed and calculated intensities of the individual points along the Bragg rod profile of the observed reflections and the weight w is the inverse of the estimated standard deviation of I_o. The variation in R_w for the monolayers as a function of ϕ is significant (Figure 2a and b). From this curve and from comparison of the observed and calculated ratios of $I_{\{0,2\}}:I_{\{1,1\}+\{1,\bar{1}\}}$ (0.295 vs 0.157, Table 2), we tend to dismiss the structure in plane group *c*1*m*1, which is a special case of *p*1*g*1 when the angle of rotation of the molecular chain is at $\phi = 90°$ (see Scheme 1a).

The Bragg rod data does not allow us, however, to distinguish between plane groups *c*1 and *p*1*g*1, because the fit indices R_w for the two plane groups are almost the same for all values of the angle ϕ (Figure 2a). The minimum value of R_w occurs for either of the structurally different orientations $\phi \approx 35°$ and 215° (as well as for their mirror images, $\phi \approx 145°$ and 325°) shown in Figure 2a–c. Thus the Bragg rod data also do not allow us to distinguish between a particular structure and its 180° rotational counterpart about the molecular axis. A calculated lattice energy profile as a function of the rotation angle ϕ provides complementary information to the results of the Bragg rod analysis. The energy curve (Figure 2d) allows us to rule out plane group *c*1, the arrangement being less stable than *p*1*g*1 by about 2 kcal/mol (or *ca.* 3 times the thermal energy, $RT \sim 0.6$ kcal/mol) at the minimum-energy arrangements corresponding to $\phi \approx 35°$ and 215°. Moreover, the plane group *c*1 is unlikely, because the packing arrangement of the chains with $\phi = 35°$ (Scheme 1e) does not involve any molecular symmetry element which would justify the observed rectangular cell.[33] Finally, as mentioned earlier, the cell dimensions projected along the molecular chain, $a_p = 4.98$ Å and $b_p = 7.42$ Å, are fingerprint evidence in favor of the orthogonal ($O_\perp$) motif in plane group *p*1*g*1. But there is still one remaining ambiguity: the calculated energy difference of about 0.5 kcal/mol between the two minimum-energy states

(34) Weinbach, S. Manuscript in preparation.

(35) Only such a distortion from pure glide symmetry can retain a unit cell angle γ of 90°, consistent with the GID data. The vector perpendicular to such a distorted glide plane lies parallel to the *ac* plane, which would be consistent with retention of a rectangular cell. After such operation, the *tilt* angle of the molecular chain from the vertical can be expressed as $\cos(tilt) = \cos(t)\cdot\cos(\delta)$. Distortion from pure glide symmetry by rotation of all the molecules, and concomitantly the "glide" plane, about the vertical axis by an angle, say δ, would induce an angle δ between the *a* axis and the vector perpendicular to the *pseudo* glide plane. Such a distortion would impose no intrinsic constraint on the unit cell angle γ to retain a value of 90°.

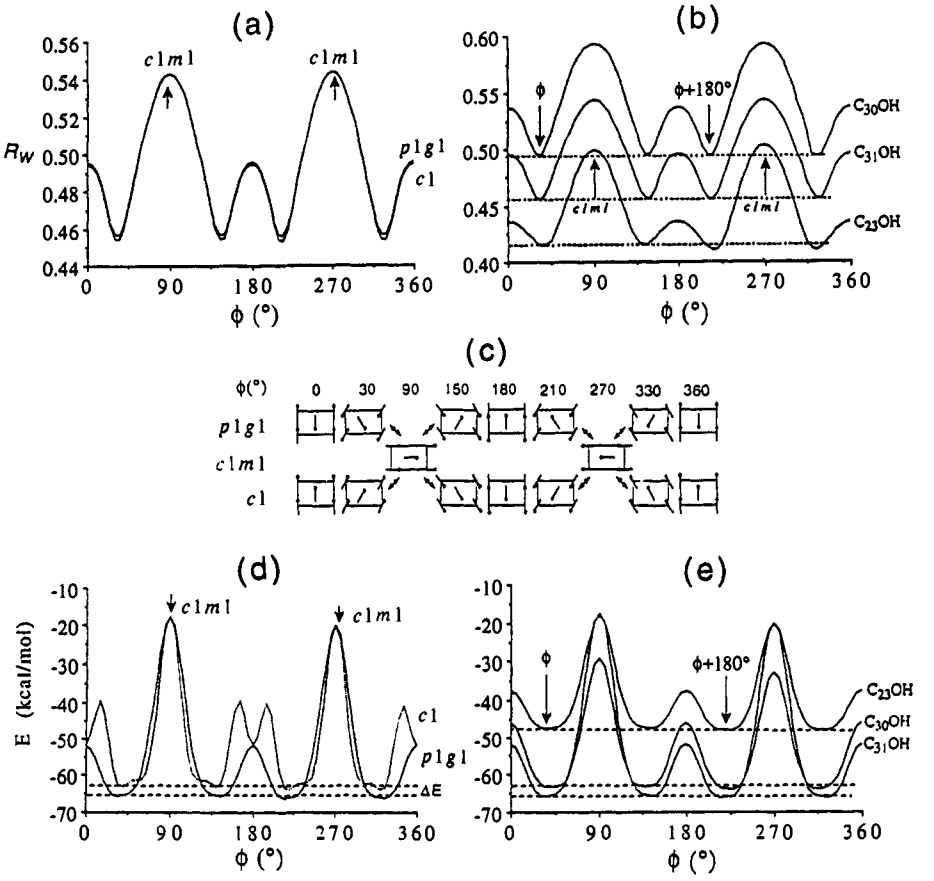

Figure 2. (a) Reliability index R_w of the 2D crystal structure of $C_{31}H_{63}OH$, as a function of rotation in ϕ of the molecule about its chain axis, for different molecular arrangements in different plane groups. The latter include $p1g1$, $c1m1$ (a special case of $p1g1$ when $\phi = 90°$), and $c1$. The curves for $p1g1$ and $c1$ almost coincide. (b) The same as in part a, for all three alcohol monolayers, but excluding plane group $c1$. The R_w index for plane group $c1m1$ is indicated as well as the positions for which R_w is minimum. Note that the crystal structures for $\phi = 90° \pm \Delta\phi$ and $270° \pm \Delta\phi$ are identical. (c) Views along the molecular axis of the structures corresponding to various ϕ values, for the plane groups $p1g1$ and $c1$ (which both become $c1m1$ for $\phi = 90°$ or 270°). The molecules have a tilt to the direction of the b axis. (d) Calculated lattice energy profiles of the $C_{31}H_{63}OH$ monolayer crystallite as a function of rotation about ϕ, the molecule with an all-*trans* conformation for the $c1$ (dotted line) and $p1g1$ (solid line) plane groups. The energy differences ΔE between the minima of the two plane groups are 1.4, 1.2, and 2.4 kcal/mol for the alcohol monolayers $C_nH_{2n+1}OH$, n = 23, 30, 31, respectively. (e) The same as in part d, but for plane group $p1g1$ only, for all the three alcohol monolayers. The minimum-energy positions at $\phi = 35°$ and 215° are indicated. Note the labels $C_{23}OH$, $C_{30}OH$, and $C_{31}OH$ represent $C_nH_{2n+1}OH$, n = 23, 30, 31, respectively.

at $\phi \approx 35°$ and 215° in plane group $p1g1$ (Figure 2e) is too low to pinpoint the actual structure.

3.2. Refinement of the 2D Crystal Structures using the GID Data. The fit of the calculated to the observed Bragg rod profiles for the three monolayers assuming plane group $p1g1$ is shown in Figure 3 (dashed line). There appears to be distinct room for improvement of the calculated Bragg rod profiles. We have assumed the molecules pack in plane group $p1g1$ of perfect symmetry. But is such an assumption justified for a monomolecular layer on the water surface? Thus we relaxed the glide symmetry of the crystal by tilting all the molecules by the same angle δ about an axis parallel to b and which lies halfway between adjacent glide planes (Scheme 2).[35]

The pseudo glide model with values of the angle δ = 1.2, 1.7, and 1.7° for the alcohol monolayers $C_nH_{2n+1}OH$, n = 23, 30, 31, respectively, yielded,[36] especially for the alcohols n = 30 and 31, a distinct improvement in the reliability indices R and R_w (Table 3) and also in the Bragg rod fits as illustrated in Figure 3. The calculated lattice energies of these pseudo glide models differed by no more than ±1 kcal/mol from those of the pure glide. Thus the deduced plane group is $p1$ with two crystallographically independent molecules per unit cell (Figure 4). A similar relaxation in glide symmetry was deduced for the uncompressed monolayers of the carboxylic acid[7] $C_{29}H_{59}CO_2H$ over water at a temperature of about 5 °C. The hydrocarbon chains of the three alcohol monolayers are arranged in the orthogonal $O_\perp$ motif with an average angle η of 86° (Table 3b) between the planes of the pseudo glide-related molecules (Figure 4). This angle is close in value to that found in the 3D crystal structure of the alcohol $C_{24}H_{49}OH$ (see section 6.3).

The Bragg rod fitting was insensitive to variation in U_z, the molecular thermal vibrational factor along the z direction, in the range 0.05–2 Å^2. This is because the molecules are aligned almost vertically, so that the intensity of the Bragg rods falls off rapidly at low q_z. Thus U_z was arbitrarily set at a value of 0.5 Å^2. On the other hand, a reliable value for the inplane thermal vibrational parameter U_{xy} for each alcohol monolayer could be extracted from the Bragg rod data, because the three observed reflections are distributed over a sufficiently large range in q_{xy}. Refinement yielded U_{xy} values of 0.07, 0.04, and 0.08 Å^2 for the three alcohols $C_nH_{2n+1}OH$, n = 23, 30, 31, respectively, as shown in Figure 5 for n = 30, 31. The average value of 0.07 Å^2 is in the same range as that obtained for the hydrocarbon chains in the 3D crystal structures of *N*-(2-hydroxyethyl)octadecanamide[37] $(CH_3(CH_2)_{16}CONH(CH_2)_2OH)$ and *n*-hexatriacontane[38] (n-$C_{36}H_{74}$) at room temperature.

The structure refinement of the three alcohol monolayers does allow us to extract a reliable measure of their relative amounts of crystalline material on the water surface because the GID

(36) As in the case for the pure glide symmetry, the molecular orientation was optimized by rotating the molecule about the ϕ axis.

(37) Dahlén, B.; Pascher, I.; Sundell, S. *Acta Chem. Scand.* **1977**, *A31*, 313–320.

(38) Boistelle, R.; Simon, B.; Pépe, G. *Acta Crystallogr.* **1976**, *B32*, 1240.

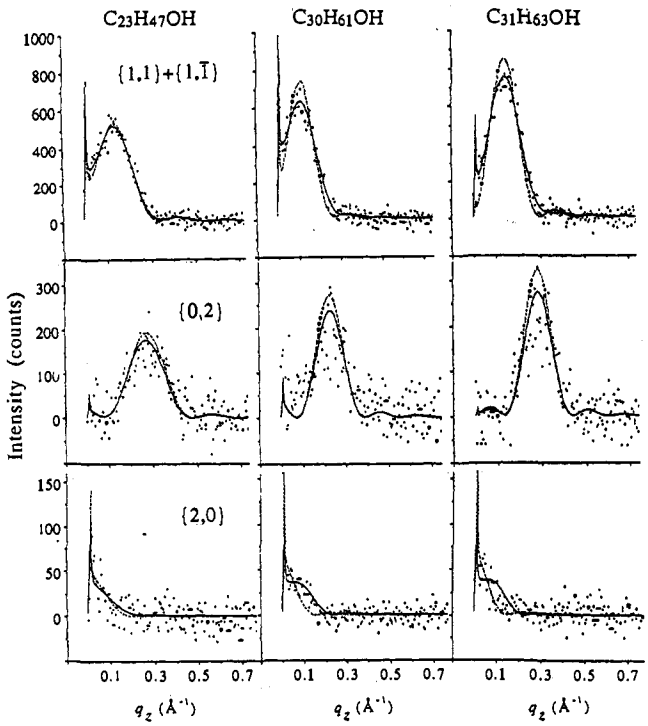

Figure 3. Observed and calculated Bragg rods of the {1,1} + {1,1̄}, {0,2}, and {2,0} reflections of the alcohol monolayers ($C_nH_{2n+1}OH$, n = 23, 30, 31), assuming an all-*trans* molecular conformation and *p*1*g*1 (dotted line) and *pseudo p*1*g*1 (solid line) plane symmetry.

Scheme 2

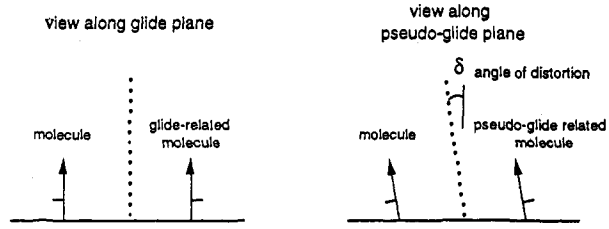

measurements were made under similar experimental conditions. We make use of the equation $I^c_{hk}(q_z) = KI^o_{hk}(q_z)$, where $I^c_{hk}(q_z)$ the calculated Bragg rod intensity derived from eq 1, is scaled to the observed value $I^o_{hk}(q_z)$ by the factor K. The derived values of $1/K$ for the three monolayers (1, 0.79, 0.99 for n = 23, 30, 31, respectively) provide a measure of their relative amounts of crystallinity.[39]

3.3. Analysis of the Head-Group Conformation. Here we shall review the various structural characteristics of 3D crystal structures of alcohols and diols in connection with the conformational and packing properties of the alcohol monolayers. Molecules of the alcohol *n*-$C_{24}H_{49}OH$ adopt an all-trans conformation in the solid state and are interlinked at one end by an O–H···O hydrogen bond (Figure 6). This is also true for the molecules of the diol $HO(CH_2)_{10}OH$, which are interlinked at both ends by hydrogen bonds (Figure 7). The molecules are respectively tilted at an angle of 36° and 46° from the normal to the layer. By comparison, in the 3D crystal structure[8,11] of $C_{17}H_{35}OH$, every other molecule exhibits a gauche conformation of the C_α–OH group about the C_β–C_α bond, and in the crystal structure of $HO(CH_2)_9OH$ (Figure 8), one end of each molecule adopts a C_α–OH gauche conformation about the C_β–C_α bond. In these two latter crystal structures the molecules are aligned vertically with respect to the layer plane. They form both intra- and interlayer O–H···O hydrogen bonds between molecules of unlike end-of-chain gauche and trans C–OH conformations.

In view of the fact that the chains of $C_nH_{2n+1}OH$ (n = 23, 30, 31) in the monolayers are tilted from the vertical by an angle as low as 9°, it was necessary to examine whether these molecules do not adopt a layer arrangement akin to that of $C_{17}H_{35}OH$ or $HO(CH_2)_9OH$. Thus we constructed analogous arrangements for the three alcohol monolayers by inserting a C–OH gauche conformation for the molecule in the center of each unit cell, as shown in Figure 9. There was little change in the calculated intensity profiles of the Bragg rods of the three observed reflections, although the model yields a weak calculated {0,1} reflection, which was not observed (Table 2). The calculated lattice energies of these models are about 1 kcal/mol less stable than those of the corresponding structures with all-trans conformations (Table 3c). This energy difference is in addition to a higher intramolecular energy, of 0.4 kcal/mol, of the gauche conformer, according to a calculation using published molecular force field parameters.[40]

The monolayer structures with the gauche-trans molecular model suffer from two drawbacks, as reflected in the higher lattice energy vis-à-vis the all-trans molecular model. One involves the poor intermolecular contacts between methyl groups at the exposed surface of the monolayer, because the methyl groups of molecules with all-trans and end-of-chain gauche conformers differ in height by about 1.2 Å (Figure 9a). This inherent disadvantage does not come into play in the 3D crystal structure of $C_{17}H_{35}OH$, because of the presence of van der Waals interlayer contacts. The other drawback involves contacts at the hydroxyl end of the molecule. As we observe in Figure 9b, the arrangement does contain a favorable O–H···O hydrogen bond (labeled d_1) of length 2.9 Å

Table 3. Results of the Bragg Rod Fitting and Packing Energy Calculations for the Alcohol ($C_nH_{2n+1}OH$, n = 23, 30, 31) Monolayers[a]

	$C_{23}H_{47}OH$	$C_{30}H_{61}OH$	$C_{31}H_{63}OH$
(a) All-trans Molecular Conformation in the Crystal with Pure *p*1*g*1 Glide Symmetry			
t (deg)	9.4	7.8	9.7
tilt	9.4	7.8	9.7
η (deg)	107.0	112.8	113.6
R	0.31	0.40	0.36
R_w	0.41	0.49	0.46
E (kcal/mol)	–48.1	–63.3	–66.1
E' (kcal/mol)	–47.7	–63.0	–65.7
(b) All-trans Molecular Conformation with Pseudo *p*1*g*1 Glide Symmetry			
δ (deg)	1.2	1.7	1.7
t (deg)	9.3	8.0	9.8
tilt	9.3	8.0	9.8
η (deg)	90.0	86.0	82.0
R	0.30	0.34	0.28
R_w	0.40	0.42	0.38
E (kcal/mol)	–48.2	–64.1	–65.7
E' (kcal/mol)	–47.4	–63.4	–64.7
(c) As in Part b, but with 50% of the Molecules Having a Gauche C_α–OH Conformation			
δ (deg)	1.1	1.7	1.6
t (deg)	9.6	7.9	9.9
tilt (deg)	9.7	8.1	10.0
η (deg)	84.0	84.0	88.0
R	0.30	0.34	0.28
R_w	0.40	0.42	0.38
E (kcal/mol)	–47.2	–62.7	–64.7
E' (kcal/mol)	–47.0	–62.1	–64.6

[a] t = angle of tilt of the molecular chain from the vertical to the direction of the b axis.[23] δ = angle of distortion of the glide plane as defined in Scheme 2. *tilt* = total tilt angle of the molecular chain from the vertical.[35] η = Dihedral angle between the molecular planes of two molecules related by (pseudo) glide symmetry, subtended along the a axis, so $\eta = 180° - 2\phi$, where ϕ is defined in the text. R and R_w are the fit indices: $R = \Sigma|I_o - I_c|/\Sigma I_o$; $R_w = \Sigma w|I_o - I_c|/\Sigma wI_o$. E = the crystal lattice energy corresponding to the minimum R_w value. E' = the crystal lattice energy with the molecule rotated by 180° about its chain axis.

(39) A firm conclusion as to the relation between chain length and extent of crystallinity for the $C_nH_{2n+1}OH$ systems requires extensive GID measurements for values of n in the range 16–31.

(40) Allinger, N. L. *J. Am. Chem. Soc.* **1977**, *99*, 8127.

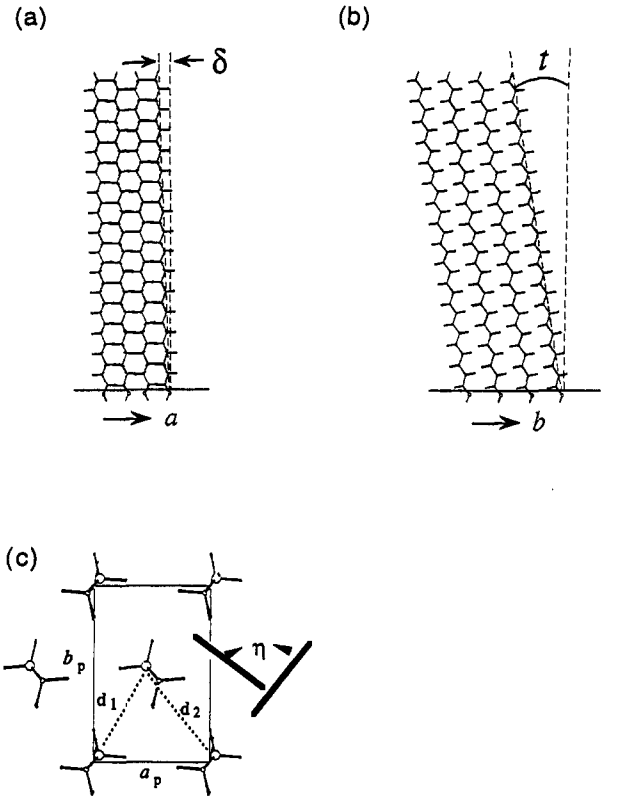

Figure 4. Structure of the alcohol monolayers $C_nH_{2n+1}OH$ (n = 23, 30, 31) in *pseudo* p1g1 symmetry. The angle of distortion of the *pseudo* glide plane δ = 1.2°, 1.7°, 1.7°; the tilt angles t to the direction of the b axis are 9.2°, 7.8°, 9.7°; the dihedral angles $\eta = 180° - 2\phi$ are 90, 86, 82° for n = 23, 30, 31, respectively; the O···O distances between *pseudo* glide related molecules i n the unit cell are d_1 = 4.2 Å, d_2 = 4.8 Å for all three monolayers: (a) view along the b axis; (b) view along the a axis; (c) view along the molecular chain axis. Note that a_p and b_p represent the unit cell a and b axes projected onto a plane perpendicular to the molecular chain axis.

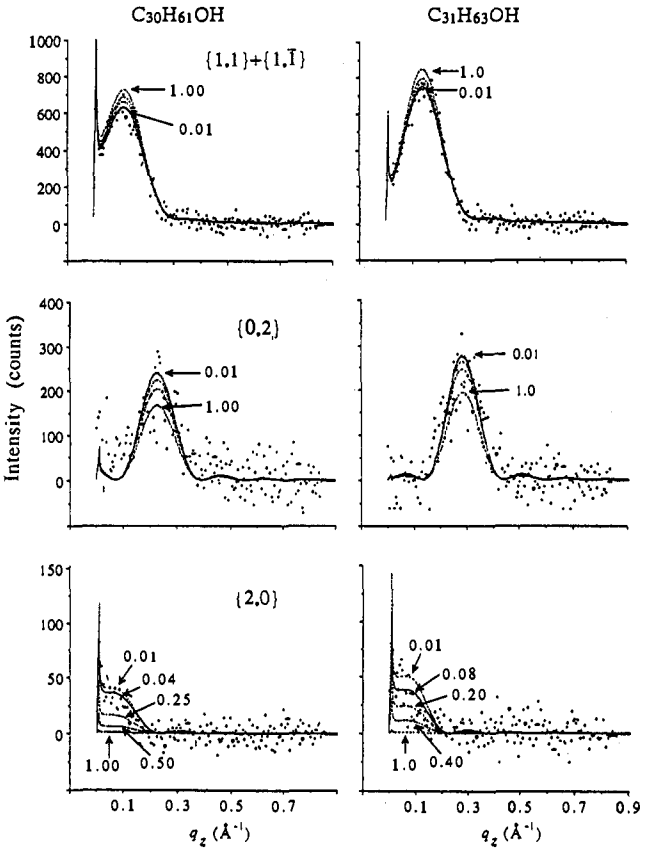

Figure 5. Observed Bragg rod intensity profiles of the {1,1} + {1,1̄}, {0,2}, and {2,0} reflections of the $C_{30}H_{61}OH$ and $C_{31}H_{63}OH$ monolayers and the variation in the calculated profiles as a function of the in-plane temperature parameter U_{xy}. This parameter was given five values ranging from 0.01 to 1.00 Å^2 for each monolayer. The symmetry of the plane group is *pseudo* p1g1. The temperature parameter U_z, along the vertical axis, was set at U_z = 0.5 Å^2.

between the gauche and trans conformers related by the pseudo glide. But the arrangement also contains a non-hydrogen-bonded contact between oxygen atoms (labeled d_2) of 3.4 Å. This contact is made through the lone-pair electrons of the two oxygen atoms and is thus weakly repulsive.[41] We may avoid this weakly repulsive interaction by an appropriate rotation of the OH bond of the molecule with the end-of-chain trans conformer, as shown in Figure 9c. Alternatively, the repulsive O···O contact in Figure 9b may be averted by adopting the alternative gauche conformation shown in Figure 9d. But the O–H···O distance (d_1) would be too long at 3.4 Å for a hydrogen bond. Surprisingly an analogous arrangement is found in the hydrogen-bonding layer structure of $HO(CH_2)_9OH$, but here the O–H···O distance is 2.74 Å, suitable for hydrogen bonding (Figure 8). This is made possible because the a axis, which is parallel to the O–H···O bond, is 6.88 Å (Table 4a), namely 0.6 Å shorter than the corresponding b axis of the monolayer structures. Nevertheless, these 2D structures have a serious drawback when we consider interaction with the underlying solvent water molecules. When a water molecule makes simultaneous hydrogen bonds with two neighboring OH groups, the distance between these two oxygen atoms is in the range 4.6 Å (Scheme 3). The monolayer packing arrangement with the all-trans conformation is ideally suited for such a condition because the distances between the oxygen atoms are 4.2 and 4.8 Å and the lattice translation is 5.0 Å (Figure 4). The arrangement of oxygen atoms in the trans-gauche model (Figure 9b,c), contains O···O distances of 2.9, 3.3, and 5.0 Å,

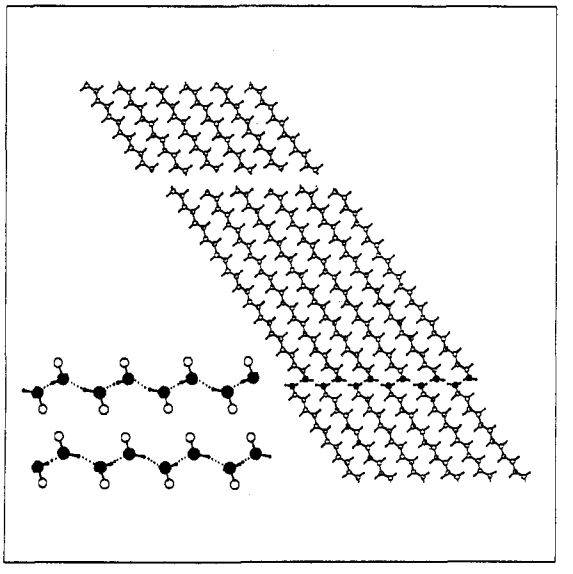

Figure 6. Packing arrangement of 1-tetracosanol ($C_{24}H_{49}OH$), showing contacts between methyl groups and between hydroxy groups (for convenience, only part of the chains of the top and bottom layers is shown). Note the disordered locations of the hydroxyl H atoms bonded to the O atoms (O). But within any hydrogen-bonding chain, the hydroxyl H atoms cannot be disordered, as shown in the insert. Thus, two different hydrogen-bonding chains, corresponding to each of two disordered H locations, coexist in the crystal.

which would be less satisfactory for hydrogen bonding to a layer of water molecules.

(41) Wang, J. L.; Berkovitch-Yellin, Z.; Leiserowitz, J. *Acta Crystallogr.* **1985**, *B41*, 341–348.

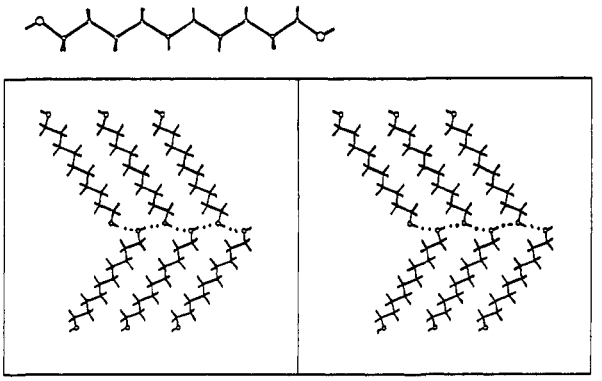

Figure 7. (Top) Molecular structure of 1,10-decanediol. (Bottom) Stereoscopic view of the molecular packing arrangement, showing interlayer hydrogen bonding.

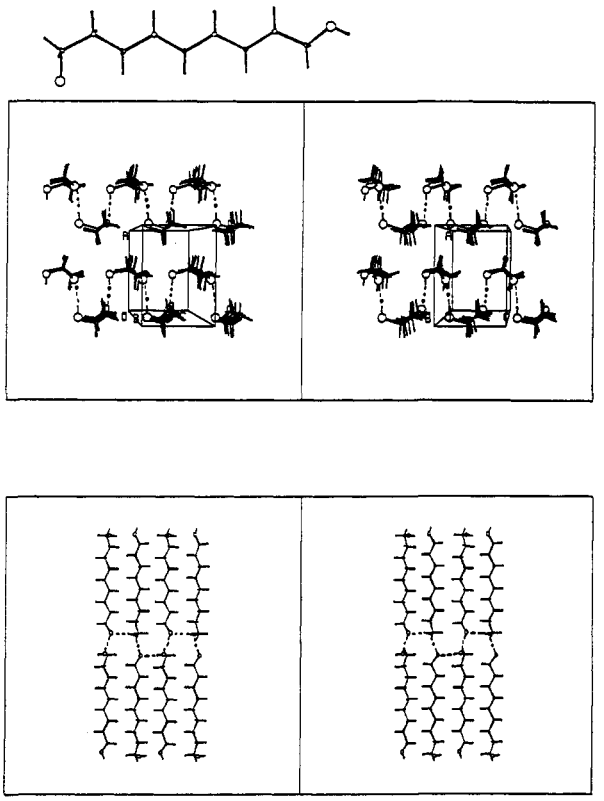

Figure 8. (Top) Molecular structure of 1,9-nonanediol. (Middle) Stereoscopic view along the *b* axis of the molecular packing arrangement, showing intralayer hydrogen bonding. (Bottom) Stereoscopic view along the *a* axis of the molecular packing arrangement, showing intra- and interlayer hydrogen bonding.

Supporting evidence for the preference of the all-trans molecular model also comes from the ice-nucleation experiments, involving monolayers of the long-chain alcohols which, when spread on drops of water, act as efficient ice nucleators.[1,13] There is certainly a better structural match between the arrangement of alcohol OH groups for the all-trans conformers than for the mixed all-trans and C–OH gauche conformers, as is evident from Figure 10. This observation is in good agreement with the fact that the crystals of $HO(CH_2)_9OH$, whose hydrogen-bonding layer structure (Figure 8) contains a mixture of trans and gauche end groups, proved to be very poor ice nucleator. Drops of water deposited upon the hydrophilic (010) face of plate-like crystals of $HO(CH_2)_9OH$ froze only upon cooling the crystals down to a temperature as low as −15 °C.[13] On the basis of all this evidence, we may dismiss the mixed all-trans and C–OH gauche model.

The ice-nucleation experiments may also be invoked to resolve the ambiguity discussed in section 3.1 regarding the azimuthal orientation of the molecules about their chain axes, as expressed

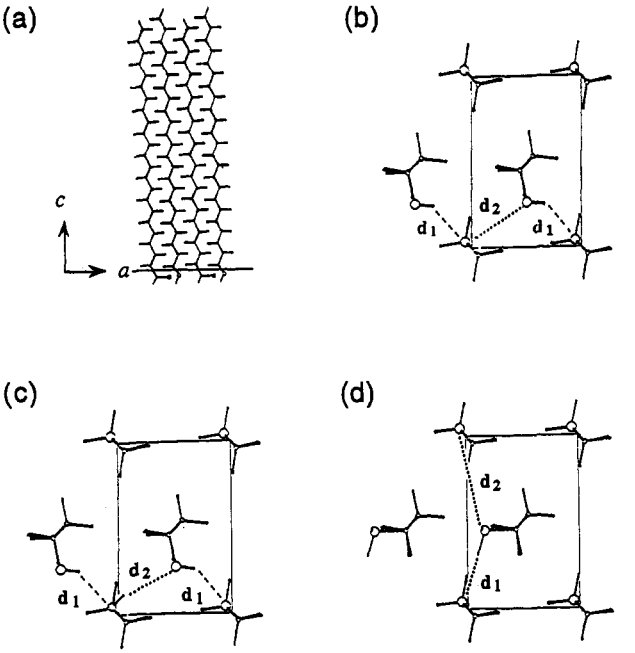

Figure 9. Possible molecular packing arrangements of alcohol monolayers ($C_nH_{2n+1}OH$, n = 23, 30, 31) with half the number of molecules with their C_α–OH groups in the *gauche* conformation about the C_β–C_α bond: (a) view along the *b* axis showing the poor molecular contact between the methyl groups at the top of the monolayer; (b) view along the molecular axis, showing different O···O distances d_1 and d_2, which are of lengths 2.9 and 3.3 Å, respectively, for all three monolayers; (c) the same as in part b, but the O–H bond of the all-*trans* conformer has been adjusted so as to form a long O–H···O contact with the oxygen atom of the *gauche* conformer; (d) packing arrangement with the alternative C_α–OH *gauche* conformation, yielding O···O contacts almost parallel to the long *b* axis. The two different O···O distances are d_1 = 3.4 Å and d_2 = 4.5 Å for all three monolayers.

in terms of the angle ϕ. The lattice energy calculations indicate that the 2D arrangements of $C_nH_{2n+1}OH$ (n = 30, 31) are the same from the hydroxyl head group up along the chain, so that a difference between the crystal structures of n = 30 and 31 manifests itself in the position of the terminal methyl group. But the energy difference between the two orientational states ϕ = 35° and 215° is as low as 0.5 kcal/mol. The ice-nucleation experiments do not yield information as to the absolute orientation of the molecular chains. But we interpret the differences in freezing point induced by the odd and even series as indicating that the positions of the OH groups of the n even and odd series are different and subsequently that the azimuthal orientations of the chains of the n odd and n even series should not differ in ϕ. Thus, if we assume, on the basis of the best fit of the observed and calculated Bragg rod intensity profiles, that ϕ = 229° for the structure of the monolayer of $C_{31}H_{63}OH$, as shown in Figure 11, then ϕ is the same for the crystal structure of $C_{30}H_{61}OH$.

4. Results on Monolayers of the $C_nH_{2n+1}CO_2C_nH_{2n}OH$ Series

4.1. Determination of the 2D Crystal Structures using the GID Data. The GID measurements are described in section 6.1. Two distinct Bragg peaks were observed, for each of the two monolayers, HDE and HNE. These Bragg peaks with their corresponding Bragg rods are shown in Figure 12. The crystallite coherence lengths L derived from the widths of the Bragg reflections,[42] are anisotropic, >1000 Å for the sharp reflection at q_{xy} = 1.68 Å^{-1}, and ~450 Å for the broader reflection at q_{xy} = 1.38 Å^{-1}. Thus both monolayers self-aggregate with a high

(42) The coherence length L associated with the hk reflections is derived from the Scherrer formula[3] $L = 0.9(\lambda/W\cos\theta)$, where W is the resolution-corrected q_{xy} line width = $(\pi/180)(\text{fwhm}^2 - \Delta q_{xy}^2)^{1/2}$ and Δq_{xy} is the resolution of the Soller collimator of width 0.007 Å^{-1}.

Table 4. Data for the Diols $HO(CH_2)_nOH$, n = 9,10 and Alcohols $C_nH_{2n+1}OH$, n = 24, 25

(a) Three-Dimensional Crystal Data

compound	1,9-nonanediol	1,10-decanediol	1-tetracosanol	1-pentacosanol
formula	$C_9H_{20}O_2$	$C_{10}H_{22}O_2$	$C_{24}H_{50}O$	$C_{25}H_{52}O$
temp (K)	300 100	100	100	100
space group	$P2_12_12_1$	$P2_1/c$	$C2/c$	$P2_1/c$
a (Å)	7.07 6.878(1)	4.799(6)	106.09(5)	4.93(2)
b (Å)	28.13 27.479(3)	5.113(3)	4.89(4)	7.10(2)
c (Å)	5.28 5.076(1)	21.029(4)	8.79(4)	135.60(3)
β (deg)		95.37(50)	91.5(3)	90.89(4)
V (Å^3)	1050 959	514	4558	4746
Z	4	2	8	8

(b) Details of Single-Crystal X-ray Diffraction Intensity Measurements and Crystal Structure Refinement

diffraction measurements			
compound	1,9-nonanediol	1,10-decanediol	1-tetracosanol
X-radiation	Mo Kα	Mo Kα	Cu Kα
temperature (K)	100	100	100
maximum 2θ measured	55	55	120
scan mode	ω	ω	ω
no. of reflections measured	2444	2634	3772
no. of independent reflections	1357	1321	1901
crystal structure refinement			
no. of parameters	186	105	202
R ($=\Sigma\|F_o - F_c\|/\Sigma F_o$)	0.044	0.064	0.118

Scheme 3

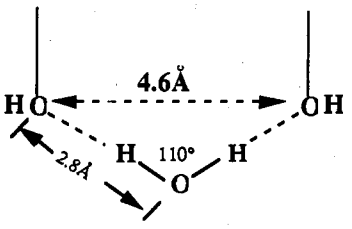

degree of crystalline order. The GID patterns of the two monolayers are similar to each other and also to that obtained from the monolayer of triacontanoic acid[7] at 5 °C, the structure of which had already been determined. Hence we could easily index the two reflections and so determine the unit cell dimensions and derive information such as plane symmetry and overall molecular packing characteristics. The two reflections at q_{xy} = 1.38 and 1.68 Å^{-1} were indexed as $\{1,1\} + \{1,\bar{1}\}$ and $\{0,2\}$, respectively, for a primitive rectangular cell, yielding the cell parameters listed in Table 5. The peak positions of the Bragg rod intensity profiles of the $\{0,2\}$ and $\{1,\bar{1}\} + \{1,\bar{1}\}$ reflections indicate that the molecules tilt at an angle t of ~29° from the vertical in the direction of the short a axis.[43] The unit cell parameters of the ab lattice projected onto a plane perpendicular to the molecular chain axis (a_p, b_p) are also shown in Table 5. They are close to the values a_p = 4.98 Å, b_p = 7.42 Å, which is a fingerprint[2,7] of hydrocarbon packing in the orthogonal $O_\perp$ motif in plane group $p11g$ for both monolayers HDE and HNE.

For the determination almost at the atomic level, of the 2D structures, we followed a procedure involving Bragg rod analysis and lattice energy calculations already described herein for the alcohols $C_nH_{2n+1}OH$.

Employing the X-ray structure factor eq 1, the intensity profiles of the Bragg rods corresponding to the two measured $\{1,1\} + \{1,\bar{1}\}$ and $\{0,2\}$ reflections were calculated using the atomic coordinate model. So as to generate all the possible arrangements with plane symmetry $p11g$, the molecules were given a full rotation in angle ϕ about their long-chain axes. The results were expressed in terms of the reliability fit indices R and R_w. The variation in R and R_w as a function of ϕ was significant. The fit of the calculated

(43) Assuming that the aliphatic tails are uniformly and rigidly tilted in the monolayer, the angle t between the molecular axis and the surface normal is given by $\cos \chi_{hk} \tan t = q_z^o/|q_{hk}|$, where q_z^o is the position of the maximum along the Bragg rod and χ_{hk} is the azimuthal angle between the tilt direction projected on the xy plane and the reciprocal lattice vector q_{hk}, as described in ref 16.

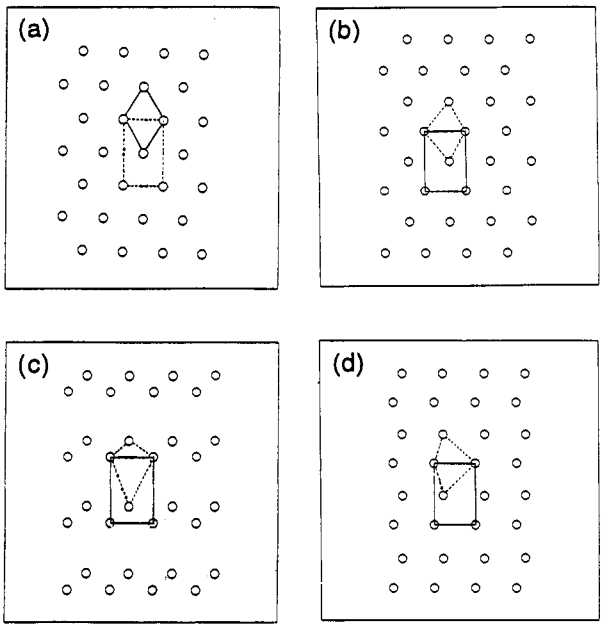

Figure 10. Layer arrangements of the oxygen atoms in the following: (a) an (001) layer of hexagonal ice; (b) the alcohol ($C_nH_{2n+1}OH$, n = 23, 30, 31) monolayers containing an all-*trans* conformation of the molecular chain; (c and d) the alcohol monolayers in which half the number of molecules adopt an end-of-chain *gauche* C_α–OH conformation about the C_β–C_α bond (cf. Figure 9). The ice lattice is depicted in terms of the regular hexagonal cell (solid line), $a_H = b_H$ = 4.5 Å, γ_H = 120°, and a centered rectangular cell (dotted line), $a_R = a_H + b_H$ = 4.5 Å, $b_R = b_H - a_H$ = 7.79 Å, γ_R = 90°. The regular rectangular lattice of the alcohol monolayers whose dimensions are given in Table 1 is drawn as well as a distorted hexagonal net joining the oxygen atoms.

to the observed Bragg rod profiles for the lowest value of the reliability index R_w (Table 6a) is shown in Figure 13 (dotted line).

According to Figure 13 (dotted lines), there is room for improvement of the calculated Bragg rod profiles of HNE and HDE. We have assumed that the molecules pack in plane group $p11g$ of perfect symmetry. This assumption did not appear to be justified for other monolayers such as the carboxylic acid[7] $C_{29}H_{59}CO_2H$ and the three alcohols $C_nH_{2n+1}OH$ described herein, where we had relaxed the glide symmetry of the crystal by tilting all the molecules by the same angle δ about an axis parallel to the glide direction and halfway between the adjacent glide planes.

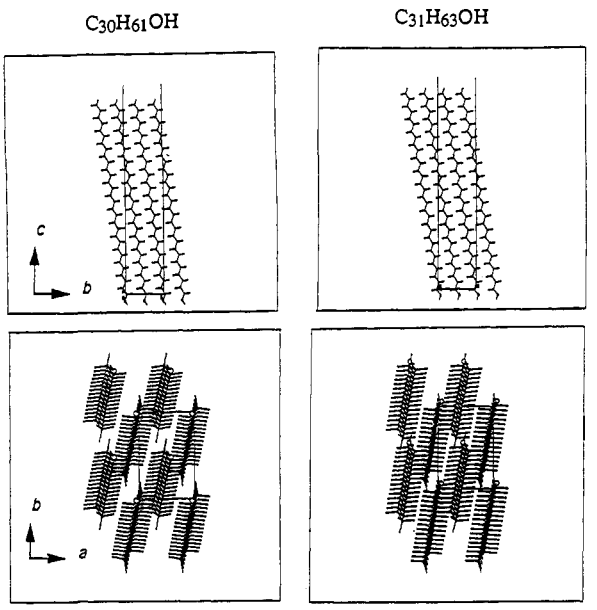

Figure 11. Views along the *a* axis (top) and the vertical *c* axis (bottom) of the molecular packing arrangements of the alcohol monolayers $C_nH_{2n+1}OH$, $n = 30$ and 31, in *pseudo p1g1* plane symmetry. The two molecules $n = 30$ and 31 do not differ in orientation about their molecular axes. This is seen in the top figure. However, the situation in which both molecules are rotated in ϕ by 180° is equally possible.

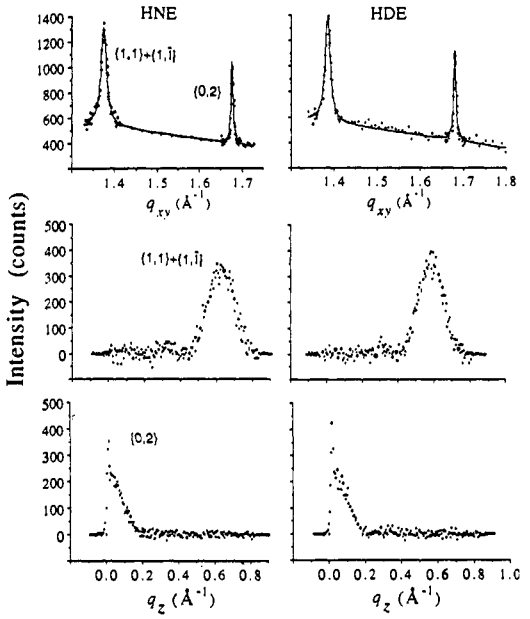

Figure 12. Observed Bragg diffraction peaks for {1,1} + {1,1̄} and {0,2} reflections across the horizontal scattering vector q_{xy} and their corresponding Bragg rod intensity profiles for the monolayers of $C_{19}H_{39}CO_2C_nH_{2n}OH$, $n = 9$ and 10, labeled HNE and HDE, respectively.

Table 5. Results of Bragg Peak Analysis for the Monolayers of HNE and HDE, i.e. $C_{19}H_{39}CO_2C_nH_{2n}OH$, $n = 9$ and 10, respectively[a]

compd	d_{11} (Å) L(Å)	d_{02} (Å) L (Å)	a (Å) (a_p)	b (Å) (b_p)	γ (deg)	A (Å^2) (A_p)	t (deg)
HNE	4.57	3.75	5.76	7.50	90	21.60	30.0
	~450	>1000	(4.99)	(7.50)		(18.71)	
HDE	4.53	3.74	5.69	7.48	90	21.28	28.0
	~450	>1000	(5.02)	(7.48)		(18.77)	

[a] The symbols t, L, a, b, a_p, b_p, and A are defined in Table 1.

Thus we applied the same relaxation to the monolayers of HNE and HDE. Best fits were obtained for δ values of 1.5° and 1.8° for HNE and HDE, respectively. The reliability index R_w shows

Table 6. Results of the Bragg Rod Fitting and Packing Energy Calculations for the Monolayers of HNE and HDE[a]

	HNE	HDE
(a) Packing Model with Pure *P*11*g* Glide Symmetry		
t (deg)	30	28
η (deg)	72	84
R	0.29	0.30
R_w	0.37	0.39
(b) Packing Model with Pseudo *p*11*g* Glide Symmetry		
δ (deg)	1.5	1.8
t (deg)	30	28
η (deg)	88	98
R	0.25	0.24
R_w	0.32	0.31

[a] t = angle of tilt of the molecular chain from the vertical in the direction of the *a* axis. The symbols δ, η, R, and R_w are defined in Table 3.

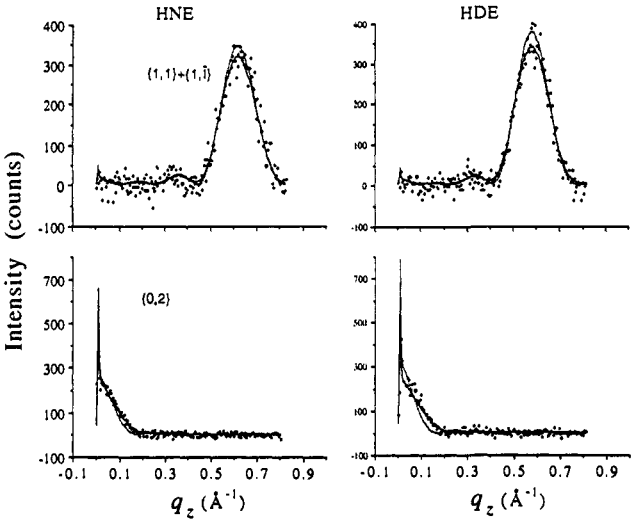

Figure 13. Observed and calculated Bragg rods of the {1,1} + {1,1̄} and {0,2} reflections of HNE and HDE, assuming *p1g1* (dotted line) and *pseudo p1g1* (solid line) plane symmetry.

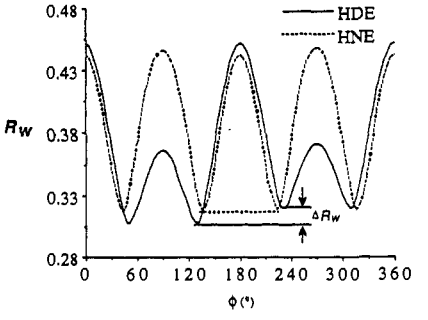

Figure 14. Reliability index R_w of the 2D crystal structures of HNE and HDE, as a function of rotation in ϕ of the molecule about its chain axis. Note that the crystal structures about $\phi = 90°$ and 270° are identical. The two different minima for HNE (dotted line), separated in ϕ by 180°, are the same, but for HDE (full line), the difference $\Delta R_w \approx 1\%$.

5–8% improvement (Table 6b) for the two structures, as manifested by the fits of the calculated Bragg rod intensity profiles illustrated in Figure 13 (solid line). For the pseudo glide model, the molecules were also given a full rotation about their chain axes. The variation in R_w for the monolayers as a function of ϕ is significant, as shown in Figure 14. However, the Bragg rod data hardly allow one to distinguish between a structure and its 180° rotational counterpart.

In these Bragg rod calculations, on the monolayers of HNE and HDE, we assumed a temperature factor of 1 Å^2 for U_z and 0.1 Å^2 for U_{xy}. The value of 1 Å^2 for U_z was taken from a GID analysis of tricontanoic acid over pure water,[7] where the molecular tilt was about 30° from the vertical. The value of 0.1 Å^2 was

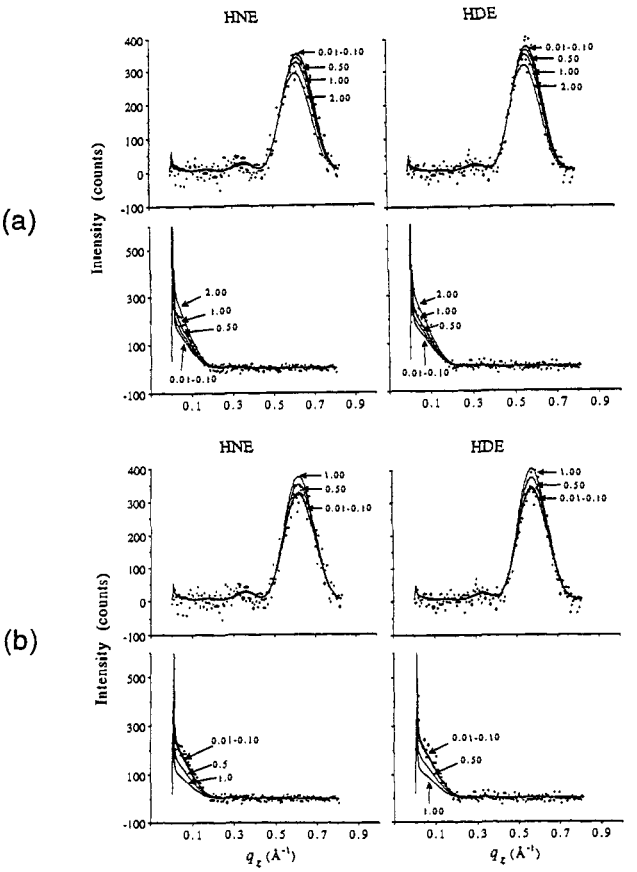

Figure 15. Observed Bragg rod intensity profiles of the $\{1,1\} + \{1,\bar{1}\}$ and $\{0,2\}$ reflections of HNE and HDE monolayers and the variation in the calculated profiles as a function of the out-of-plane (U_z) and in-plane (U_{xy}) temperature parameters. These parameters were each given five values ranging from 0.01 to 2.00 Å^2 for each monolayer; the solid line shows the best fit profile. The symmetry of the plane group is pseudo $p11g$: (a) variation in U_z, keeping U_{xy} fixed at 0.1 Å^2; (b) variation in U_{xy}, keeping U_z fixed at 1 Å^2.

taken from the analysis of the alcohols $C_nH_{2n+1}OH$, n = 23, 30, 31 and from an analysis of the GID data of the monolayer of triacontanoic acid ($C_{29}H_{59}CO_2H$) over $CdCl_2$ solution at high pH,[44] which yielded $U_{xy} \approx 0.08 \pm 0.03$ Å^2, an estimate made possible by four observed Bragg rods spanning q_{xy} in the range 1.54–1.84 Å^{-1}. The molecules in this 2D crystal structure are aligned almost vertical to the water surface. On the reasonable assumption that the in-plane U_{xy} motion of HNE and HDE should be in the same range as that of the long-chain alcohols C_nH_{2n+1}-OH (n = 30, 31), we examined the effect of varying U_z on the Bragg rod profiles but keeping U_{xy} fixed at 0.1 Å^2. The results (Figure 15a) show that a good fit is obtained for a U_z value of 1 Å^2. Limiting U_z within the range of 0.5–1.0 Å^2, U_{xy} was varied. A good fit was obtained for $U_{xy} \approx 0.1$ Å^2 (Figure 15b) but not when U_z was set lower than 0.5 Å^2. Although it is obvious from Figure 15 that U_{xy} and U_z are strongly correlated, the derived values are reasonable on the basis of the measured data for the normal long-chain alcohols and acids.

4.2. Lattice Energy Calculations. As already mentioned, one ambiguity remains from the Bragg rod analysis of HNE and HDE (Figure 14); structures which differ only in axial rotation by 180° give the same reliability index R_w. To help overcome this ambiguity, lattice energy calculations were performed on the same ensemble of crystal structures as generated for the Bragg rod analysis. For convenience, we assumed that the structure is arranged in the perfect plane symmetry $p11g$.

(44) Bohm, C.; Leveiller, F.; Jacquemain, D.; Mohwald, H.; Kjaer, K.; Als-Nielsen, J.; Leiserowitz, L. *Langmuir*, in press.

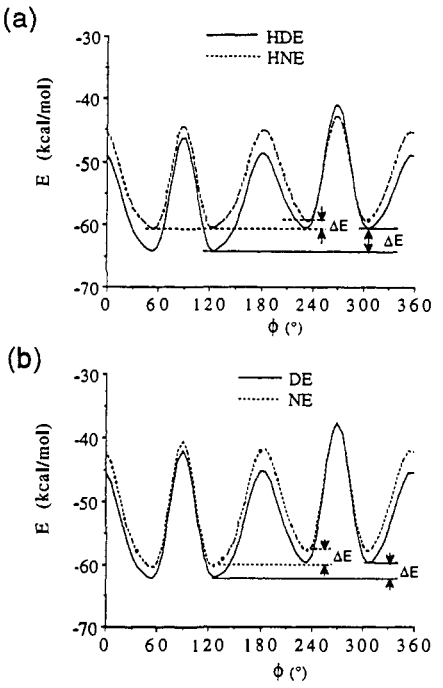

Figure 16. (a) Calculated lattice energy profiles of the monolayer crystallites of HNE and HDE (i.e. $C_{19}H_{39}CO_2H_{2n}OH$, n = 9, 10, respectively) as a function of rotation about ϕ. Note the pure $p11g$ glide symmetry is assumed. The energy differences ΔE between the minima of the two monolayers are 1.2 and 3.6 kcal/mol for HNE and HDE, respectively. (b) The same as in part a, but for the NE and DE (i.e. $C_{19}H_{39}CO_2C_nH_{2n}H$, n = 9, 10, respectively) models. ΔE values between the minima of the two monolayers are 2.6 and 2.5 kcal/mol for NE and DE, respectively.

The lattice energy profiles for HNE and HDE are shown in Figure 16a. The two energy minima for both HNE and HDE located at ϕ = 54° and 234° differ by ΔE = 1.2 kcal/mol for HNE and 3.6 kcal/mol for HDE. For both systems the lower energy is at ϕ = 54°. The energy profiles are plotted in Figure 16b for the analogous molecules which bear no OH group, namely the alkyl esters of *n*-nonyl eicosanoate (NE) and *n*-decyl eicosanoate (DE). Their energy profiles follow the same pattern as those of HNE and HDE, but ΔE is ~2.6 kcal/mol for both systems. There is no doubt that the contributions of the NE and DE moieties of HNE and HDE, respectively, favor the same molecular orientation, at ϕ = 54°. The additional OH group has a modifying influence; nevertheless, the energy differences still point to the same orientation for both monolayers. Therefore it is possible to fix the correct molecular orientation for pseudo glide symmetry from the Bragg rod analysis shown in Figure 14, leading to ϕ = 44° and 49° for HNE and HDE, respectively. Their packing arrangements are shown in Figure 17.

4.3. Correlation between Crystalline Coherence Length and Energy of Attachment. There is a pronounced difference in the crystal coherence length L associated with the $\{1,1\} + \{1,\bar{1}\}$ and $\{0,2\}$ reflections of HNE and HDE (Table 5). L is much smaller along the direction of molecular tilt. Triacontanoic acid ($C_{29}H_{59}$-COOH) and other fatty acids over pure water[7] were also shown to exhibit crystalline coherence lengths which were smaller along the molecular tilt direction. This anisotropy of triacontanoic acid was accounted for in terms of the difference in the attachment energy (E_{att}) of different (h,k) rows of molecules to the crystal, the logic being that the lower the attachment energy, the easier it is to disturb or disrupt the crystal about the (h,k) line. This effect should be more pronounced in systems exhibiting molecules with large tilt angles. The results of the attachment energy calculations in the 2D crystals of HNE and HDE are listed in Table 7. The attachment energy in the b direction, corresponding to the $\{0,2\}$ reflection, is about 3 kcal/mol stronger than the

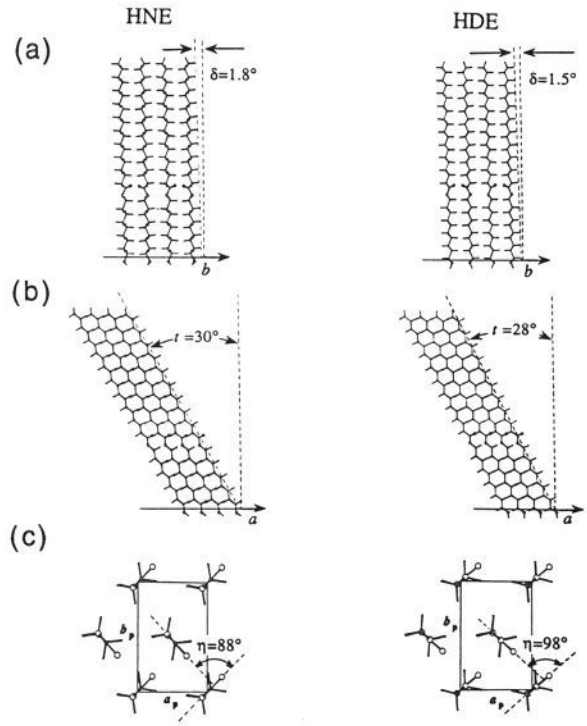

Figure 17. Structures of monolayers of the hydroxyl alkyl esters of HNE and HDE in *pseudo* $p11g$ symmetry. The angle of distortion of the *pseudo* glide plane δ = 1.8° and 1.5°; the tilt angle t from the vertical to the direction of the a axis = 30° and 28°; and the dihedral angle $\eta = 2\phi$ = 88° and 98° for HNE and HDE, respectively. Views are along (a) the a axis, (b) the b axis, and (c) the molecular chain axis. Note that a_p and b_p represent the unit cell axes a and b projected onto a plane perpendicular to the molecular chain axis.

Table 7. Energy of Attachment (E_{att}) per Molecule between the $\{h,k\}$ Molecular Layer and the Rest of the Monolayer Crystal of HNE and HDE and the Measured Coherence Lengths along These $\{h,k\}$ Directions

compound	$\{h,k\}$	E_{att} (kcal/mol)	L (Å)
HNE	{1,1}	−20.4	430
	{0,2}	−23.1	≥1000
HDE	{1,1}	−22.0	450
	{0,2}	−24.7	≥1000

attachment energy in the $a^* \pm b^*$ direction, corresponding to the $\{1,1\} + \{1,\bar{1}\}$ reflections. This result indicates that the crystal is probably more fragile along the molecular tilt direction, in agreement with the results obtained for triacontanoic acid.

5. Conclusion

The 2D crystal structures of the uncompressed monolayers of the alcohols $C_nH_{2n+1}OH$ (n = 23, 30, 31) and $C_{19}H_{39}CO_2C_nH_{2n}OH$ (n = 9, 10) over water at 5 °C have been determined at almost atomic level from the grazing incidence X-ray diffraction (GID) data and lattice energy calculations. The molecules crystallize, packing in a rectangular cell in the orthogonal $O_\perp$ motif with pseudo glide plane symmetry. It was possible to get an estimate of the molecular motion in the crystal. The Bragg rod analysis and the energy calculations support the all-trans conformation of the molecule. The analysis does not allow one to distinguish between the structure of the normal alcohols $C_nH_{2n+1}OH$ and that of its 180° rotational counterpart about the molecular axis. Nevertheless, the structure determination provides concrete evidence as to the role of a lattice and structural match for induction of ice nucleation by the long-chain $C_nH_{2n+1}OH$ alcohol monolayers[1,13] through an epitaxial mechanism.

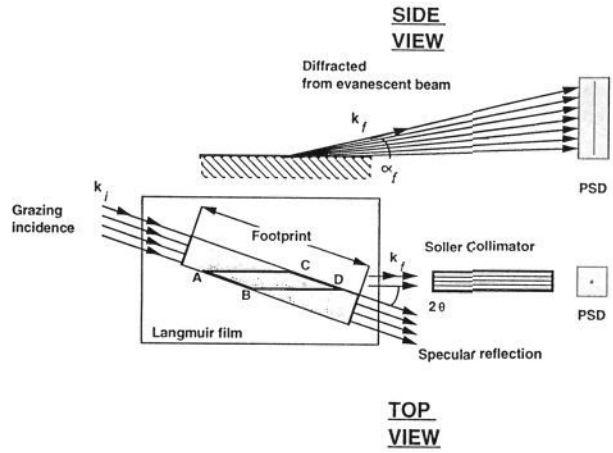

Figure 18. Top and side views of the GID geometry. The footprint of the grazing incidence beam is delineated. The position-sensitive detector (PSD) has its axis along the vertical direction. Only the area *ABCD* contributes to the measured scattering.

It was possible to determine the absolute orientation of the molecules of $C_{19}H_{39}CO_2C_nH_{2n}OH$ (n = 9, 10) by the lattice energy calculations. The anisotropy of the crystalline coherence lengths in the different crystalline directions of these two systems could be correlated with the energy of binding molecules in these directions. The orientations of the OH group of the two molecules n = 9, 10 with respect to the water surface are decidedly different. We may correlate this difference with their different ability to nucleate ice.[13]

6. Experimental Section

6.1. Grazing Incidence Diffraction Measurements from the Alcohol Monolayers. The measurements on monolayers were carried out using the liquid surface diffractometer on the synchrotron X-ray beam line D4 at Hasylab, DESY, Hamburg. A sealed and thermostated Langmuir trough equipped with a Wilhelmy balance, allowing for surface pressure control of the film, was mounted on the diffractometer. The synchrotron radiation beam was monochromated to a wave length λ = 1.39 Å by Bragg reflection from a Ge(111) crystal and, to maximize surface sensitivity, was adjusted to strike the monolayer surface at an incident angle $\alpha_i = 0.85\alpha_c$ (where $\alpha_c = 0.138°$ is the critical angle for total external reflection). This limits the penetration depth of the beam to that of the evanescent wave, and the scattering due to the subphase is efficiently reduced. This permits a reliable measurement of the weak diffraction signal originating from the crystalline monolayer.[16] The dimensions of the footprint (Figure 18) of the incoming X-ray beam on the liquid surface were 50 × 5 mm.

Chloroform solutions of long-chain alcohol $C_nH_{2n+1}OH$ (n = 23, 30, 31) and of the hydroxy alkyl eicosanoates $C_{19}H_{39}CO_2C_nH_{2n}OH$, n = 9, 10, labeled HNE and HDE, respectively, were spread on the water surface in the trough with ~75% surface coverage at room temperature. The GID data were measured for a water surface temperature of 5 °C. The collection of the diffracted radiation was made in two ways using a one-dimensional position-sensitive detector (PSD, Figure 18), which intercepted photons over a range $0.0 \le q_z \le 0.9$ Å^{-1}, mounted vertically behind a horizontally collimating Soller slit, of resolution width $\Delta(q_{xy}) = 0.007$ Å^{-1}. The scattered intensity, measured by scanning different values of q_{xy} and integrating over the whole q_z window of the PSD, yields Bragg peaks. Simultaneously, the scattered intensity recorded in channels along the PSD but integrated over q_{xy} across a peak produces q_z-resolved Bragg rod intensity profiles. Three reflections were measured for each of the three alcohol $C_nH_{2n+1}OH$ (n = 23, 30, 31) monolayers in the q_{xy} range 1.3–2.6

Å^{-1}, as described previously.[2] Two reflections were found for the HDE and HNE monolayers in the q_{xy} range 0.70–1.80 Å^{-1}.

6.2. Structure Determination of 3D Crystals of 1,9-Nonanediol and 1,10-Decanediol. The compounds 1,9-nonanediol ($HO(CH_2)_9OH$) and 1,10-decanediol ($HO(CH_2)_{10}OH$) with 98% purity were purchased from Aldrich Co. Thin (0.05 mm) plate-like crystals of these two compounds for X-ray diffraction measurements were grown from chloroform and methylene chloride solutions, respectively, by slow evaporation at room temperature. A Rigaku AFC5 diffractometer equipped with a Mo rotating anode X-ray source was used for the intensity data collection on specimen crystals cooled to a temperature of ~100 K. The crystal structures were solved by direct methods using the SHELX86 computer program.[45] All the H atoms were located from electron density difference maps. Conventional structure-factor least-squares refinement was performed using the SHELX76 program,[46] with anisotropic thermal parameters for C and O atoms and isotropic thermal parameters for H atoms. Details of crystal data, X-ray intensity measurements, and refinement are listed in Table 4. The final x, y, z coordinates, thermal parameters, bond distances, bond angles, and torsional angles are available as supplementary material.

The molecular structures and packing arrangements are shown in Figures 7 and 8. The molecular chain of 1,9-nonanediol has an all-trans conformation but for one end of the molecule where the C_α–OH bond adopts a gauche conformation about the C_α–C_β bond (torsion angle C_γ–C_β–C_α–O = –63.3°). The molecules pack in layers with the chain axes perpendicular to the layer whose area per molecule is 17.5 Å^2. These chains form the orthogonal $O_\perp$ motif[4,6] by twofold screw symmetry. The trans and gauche C–C–C–OH moieties are interlinked by O–H···O hydrogen bonds both within and between layers (Figure 8). The intralayer O–H···O distance is 2.74 Å, and the interlayer distance is 2.70 Å.

The molecule of 1,10-decanediol in its crystal structure has an all-trans conformation. It forms a layer structure in the *ab* plane by translation symmetry only (Figure 7). The molecular chains are tilted at an angle of 44.1° from the *ab* plane. The projection of the *ab* unit cell onto a plane perpendicular to the chain axis is a_s = 4.02 Å, b_s = 4.53 Å, γ_s = 70.0°. With a tilt angle of 44.1°, the hydroxyl OH groups are properly oriented to form a hydrogen-bonded chain by twofold screw symmetry along the *b* axis, with an OH···O distance of 2.80 Å, and so interlink neighboring *ab* molecular layers.

6.3. Crystal Structure Determination of 1-Tetracosanol. Compounds of 1-tetracosanol ($C_{24}H_{49}OH$) and 1-pentacosanol ($C_{25}H_{51}OH$) with purity of 99% and 98%, respectively, were purchased from Sigma Co. Thin diamond-shaped plate single crystals of these two compounds were obtained from methylene chloride solution by slow evaporation at room temperature. The X-ray reflections from a crystal cooled to a temperature of ~100 K were measured on a Rigaku AFC5 diffractometer equipped with a Cu rotating anode X-ray source. The low-temperature cell parameters of these two crystals are shown in Table 4a. Details of the intensity data collection are listed in Table 4b.

The crystal structure determination and refinement of 1-tetracosanol were essentially straightforward, although {*hkl*} reflections with *h* indices higher than 99 were not measured, because of a computer software limitation. Thus the refinement was performed by adjusting the U_{11} temperature factor of each C and O atom to be equal to the average value of its U_{22} and U_{33} terms. The methylene hydrogen atoms were introduced into their proper positions. A single peak appropriate for a position of the hydroxy hydrogen atom was located on an electron density difference map, but as discussed below, the hydroxyl hydrogen atom must be disordered. The structure was refined to an *R* value of 11.8%.

The crystal structure of 1-tetracosanol is composed of molecular layers parallel to *bc*. In the layer, the molecules which have an all-trans conformation are tilted from the normal to the *bc* layer by 36°. They pack in the orthogonal $O_\perp$ motif by glide symmetry with a dihedral angle η of 87.7° between the planes of the glide-related molecules. Between the layers, the methyl groups of the molecules make CH_3···CH_3 contacts of 3.87 and 3.95 Å across centers of inversion and twofold screw axes, respectively. At the opposite end of the molecule, the hydroxyl oxygen atoms make contacts of 2.68 Å across centers of inversion and 2.66 Å across twofold axes. Thus the hydroxyl hydrogen atoms must occupy two disordered positions with half occupancy, yielding hydrogen-bonded chains parallel to the *c* axis, as shown in Figure 6.

The very long *c* axis of the crystal of 1-pentacosanol ($C_{25}H_{51}OH$) and the slightly warped shape of the specimen plate-like crystal made it very difficult to separate neighboring X-ray reflections. We were thus not able to refine the crystal structure to proper completion.

Acknowledgment. We thank Ronit Popovitz-Biro for fruitful discussions, Ada Yonath of the Max Planck Unit for Structural Molecular Biology for use of laboratory facilities, Christine Böhm for help during the grazing incidence diffraction measurements at the synchrotron beam line, and Edna Shavit for preparation of hentriacontanol ($C_{31}H_{63}OH$). We acknowledge financial support from the Minerva Foundation, the Petroleum Research Fund from the American Chemical Society, and the Danish Foundation for Natural Sciences. We also thank HASYLAB, DESY, Hamburg, FRG, for synchrotron beam time. J.-L.W. is indebted to CSIST of Taiwan for financial support.

Supplementary Material Available: Tables of the atomic coordinates, bond lengths, bond angles, and torsion angles of 3D crystalline 1,9-nonanediol, 1,10-decanediol, and 1-tetracosanol and the atomic coordinates of the 2D crystalline monolayers of $C_nH_{2n+1}OH$ (n = 23, 30, 31) and $C_{19}H_{39}CO_2C_nH_{2n}OH$ (n = 9,10) (35 pages). This material is contained in many libraries on microfiche, immediately follows this article in the microfilm version of the journal, and can be ordered from the ACS; see any current masthead page for ordering information.

(45) Sheldrick, G. M. *SHELX-86. Program for the solution of crystal structures*; University of Göttingen: Göttingen, Federal Republic of Germany, 1986.

(46) Sheldrick, G. M. *SHELX76. Program for crystal structure determination*; Cambridge University: Cambrdige, England, 1976.